Iranian Association of Chemical Engineers, Unit 11, No. 13 (Block 3), Maad Building, Shahid Akbari Boulevard, Azadi Ave., Tehran - Iran.

Tel: +98 21 6604 2719 **Fax:** +98 21 6602 2196

Iranian Journal of Chemical Engineering

Vol. 16, No. 1 (Winter 2019), IAChE

Study on Diffusion Coefficient of Benzene and Ethyl Benzene Vapours in Nanoporous Silica Aerogel and Silica Aerogel-Activated Carbon Composites **3-21**

A. Mohammadi, J. S. Moghaddas

Synthesis of Zeolite NaA Nano-Crystals: Effect of Synthesis Parameters on Crystallinity and Crystal Size **22-38**

S. M. Mirfendereski

Optimization of Water-Based Drilling Fluid Produced Using Modified Nigerian Bentonite and Natural Biopolymers: Reduced Experiment and Response Surface Methodology **39-53**

A. O. Arinkoola, T. O. Salawudeen, K. K. Salam, M. O. Jimoh, G. O. Abidemi, Z. M. Atitebi

Experimental, Kinetic, and Isothermal Modeling of Carbon Dioxide Adsorption with 13X Zeolite in a Fixed Bed Column **54-69**

M. Khajeh Amiri, A. Ghaemi, H. Arjomandi

Comparison of Different Methods (Digestion, Combustion, Gasification, and Pyrolysis) for Sludge Energy Recovery: A Case Study for Ekbatan's Municipal Treatment Plant **70-82**

A. Hemmati, T. Abedzadegan

Prediction of the Pharmaceutical Solubility in Water and Organic Solvents via Different Soft Computing Models **83-100**

A. Yousefi, K. Movagharnejad

Comparison of the Performance of Different Reverse Osmosis Membrane Modules by CFD Modeling **101-116**

M. Bahoosh, E. Kashi, S. Shokrollahzadeh, Kh. Rostami

Notes for Authors **117**

Iranian Journal of Chemical Engineering
Vol. 16, No. 1 (Winter 2019), IAChE

Study on Diffusion Coefficient of Benzene and Ethyl Benzene Vapours in Nanoporous Silica Aerogel and Silica Aerogel-Activated Carbon Composites

A. Mohammadi, J. S. Moghaddas [*]

Transport Phenomena Research Center, Faculty of Chemical Engineering, Sahand University of Technology, P. O. Box: 51335-1996, Tabriz, Iran

ARTICLE INFO

Article history:
Received: 2017-12-26
Accepted: 2018-10-13

Keywords:
Adsorption Kinetic,
Diffusion Coefficient,
Equilibrium Adsorption Capacity,
First-Order and Second-Order Model,
Silica Aerogel

ABSTRACT

In this study, nanoporous silica aerogel and silica aerogel-activated carbon composites have been synthesized using a water glass precursor by a cost-effective ambient pressure drying method. Equilibrium and kinetics of benzene and ethylbenzene adsorption on silica aerogel and its composites have been measured in a batch mode at three weights of adsorbent. For the first time, the experimental data have been found to fit the intra-particle diffusion model for determining diffusion coefficients. The saturation adsorption capacities of benzene and ethylbenzene vapors were 2033 mg.g^{-1} and 458 mg.g^{-1}, respectively. The components uptake curves have been described by mathematical models of pseudo-first-order and pseudo-second-order models. It has been found that the pseudo-first-order model fits the experimental data better than the pseudo-second-order model. Also, the pseudo-second-order model could be used for modeling of benzene adsorption over silica aerogel and silica aerogel-2 % wt activated carbon composite at the beginning of adsorption process. The diffusion coefficients of benzene and ethylbenzene within the silica aerogel were in the range of 2.16×10^{-14} - 6.66×10^{-13} $m^2.s^{-1}$ *and* 3.65×10^{-13} - 1.95×10^{-12} $m^2.s^{-1}$, *respectively.*

1. Introduction

One of the main sources of air pollution is industrial activities. Volatile organic compounds (VOCs) are the common air pollutants resulting from industrial activities such as chemical, petrochemical, and related industries as well as motor vehicles [1-3]. BTEX is a part of VOCs easily volatilized and released into the environment because of their high vapor pressure [4]. VOCs, especially BTEX, are hazardous to human health, plants, and vegetation [5] and cause serious environmental problems such as the destruction of the ozone layer, photochemical smog, and global warming [6, 7]. Therefore, it is necessary to control and prevent these components emission [2]. Adsorption techniques are extensively used for the removal of VOCs, especially in gas/liquid pollutants with low concentrations [7, 8].

[*]Corresponding author: jafar.moghaddas@sut.ac.ir

These techniques are inexpensive to fabricate and need simple equipment for removing VOCs from gaseous streams [5]. Up to 2008, approximately 10 % of the pollution abatement units are based on adsorption. Now, this percentage has increased to attain strict control over VOCs releases set by the laws [9]. In the adsorption process, the most important parameter is the selection of appropriate adsorbents with sufficient efficiency for VOCs removal largely dependent on the chemical nature of the gaseous stream containing adsorbate [10]. Microporous [11] and mesoporous [12] adsorbents, such as activated carbon [13, 14], activated carbon fibers [15], zeolites [16], porous clay ore [17], activated alumina [18], silica gel [19-21], and/or molecular sieve adsorbents, have been mostly used to remove VOCs [8, 22]. However, in practice, common porous materials meet some disadvantages such as low adsorption capacity, flammability, slow adsorption kinetic, and other problems related to regeneration [8]. Therefore, in the adsorption process, attention is given to the selection of adsorbent with high adsorption capacity, fast kinetics, and the possibility of regeneration [8, 17]. Aerogels show some extraordinary and unique properties such as high specific area (500-1200 m^2g^{-1}) [23], high porosity (80-99.8 %) [24], low density (0.08 gcm^{-3}) [25], high thermal insulation (0.043 $Wm^{-1}K^{-1}$) [26], low dielectric constant [27], open pore 3-D network [28], and controllable porous dimensions on the nanometer scale [29]. These prominent properties make them useful materials for several applications in both science and technology such as thermal insulation [30], filters for removal of toxic compounds [31, 32], as supports for inorganic nanoparticles [33], acoustic insulation [34], space engineering [34, 35], humidity sensor [36, 37], wastewater treatment [38, 39], and adsorption because of high specific area and high porosity [40, 41]. Silica aerogels are used in the adsorption process because of high-rate and high-capacity adsorption for VOCs, especially BTEX pollutant. In spite of the widespread applications of silica aerogels, their fragility, brittleness, and weak mechanical strength, their applications are limited in various fields such as adsorption and thermal insulation [6, 42]. Therefore, it is expected that the addition of activated carbon to the aerogel matrix reinforces aerogel network, and the resulting silica aerogel-activated carbon composites may improve the adsorption performance of the adsorbent and, accordingly, reduce the cost [6]. In order to study comprehensively, adsorption performance and mechanism of fixed-bed or any other flow-through systems depending on the physical and chemical properties of the adsorbent, thermodynamic, and kinetic aspects must be considered [43, 44]. Furthermore, the modeling of adsorption processes is required to obtain an understanding of the dominant phenomenon and, consequently, designing of the process [45]. There are several mathematical models that are classified as adsorption reaction models and adsorption diffusion models. These two models are applied to describe the kinetics of the adsorption process in spite of the difference in its nature [43]. The two common and simplest mathematical models for describing the interactions of adsorbate-adsorbent and adsorption kinetic behaviors are pseudo-first-order and pseudo-second-order models [44]. Adsorption diffusion models are based on three sequential steps (1) diffusion across the external boundary layer surrounding the adsorbent; (2) intra-particle

diffusion and/or diffusion along the pore walls; (3) adsorption and desorption of adsorbate [43]. The diffusion coefficient of adsorbate is one of the factors that affects the intensity of adsorption, which has a relationship with physical properties of VOCs such as molecular size, and depends on the microstructure of VOCs such as pore size [46, 47]. The adsorption capacity of adsorbent is also significant for the pilot application besides kinetic behavior [43]. There are three methods for the measurement of adsorption capacity (adsorption isotherm) [48]:

1. Static volumetric method [49, 50]
2. Dynamic column method [40, 51]
3. Gravimetric method [8]

There is limited information in the literature relating to kinetic adsorption and diffusion coefficients of silica aerogel and silica aerogel-activated carbon composites. Therefore, in the present study, after synthesis of nanometer silica aerogel and silica aerogel-activated carbon composite using a water glass precursor by the ambient pressure drying method, the adsorption capacity of synthesized samples was determined by the gravimetric method. Then, pseudo-first-order and pseudo-second-order models were selected to study the static adsorption rate behavior (adsorption kinetic), and the intra-particle diffusion model or homogeneous solid diffusion model (HSDM) was adopted to measure the diffusion coefficient of benzene and ethylbenzene on silica aerogel and silica aerogel-activated carbon composites.

2. Experimental Procedure

2.1. Sample preparation

Silica aerogels were produced by a two-step sol-gel process followed by the ambient pressure drying. The precursor used for the preparation of hydrogels was water glass (purchased from Merck). TMCS and ion exchange resin, including Amberlite IR 120 H^+, were purchased from Merck. Other agents such as isopropyl alcohol (IPA), ammonium hydroxide solution (1.0 M), and n-hexane were kindly provided by Dr. Mojallali Chemical Complex Co. The procedure of silica aerogel production was completely reported in previous work by our research team [40].

2.2. Methods of characterization

The apparent density of the aerogel was measured based on the mass and volume. The volume of powdery aerogels was obtained by filling the powders into a graduated cylinder and tapping them at a constant speed. The mass of aerogels was measured by an accurate balance. A scanning electron microscope (SEM: JSM-6700F) was used to observe the microstructure and morphology of the aerogel samples. The specific surface areas, total pore volumes, and the pore diameters of aerogel samples were determined by nitrogen physisorption at -196 ^oC using a BET (Belsorb mini II) surface analyzer. Fourier transform infrared spectroscopy (FTIR, 4600 Unicam) was employed to confirm the existence of –OH, Si–OH, Si–O–Si, Si–C, and C–H bonds in the wave number range of 400 to 4000 cm^{-1}.

2.3. Adsorption isotherms and diffusion coefficients determination

Static adsorption kinetics and equilibrium adsorption capacity of the aerogels were determined using a Professional Analytical Balance (Mettler AT261) at three weights of 0.01, 0.02, and 0.04 g. A certain amount of adsorbent was exposed to benzene and

ethylbenzene vapors in a special container. The absorbent weight change by the absorption of benzene and ethylbenzene vapors was measured over time with an intelligent balance of 10^{-5} g accuracy.

Then, the obtained adsorption isotherms fit the theoretical fractional approach to equilibrium [47] described by Equation (1) (intra-particle diffusion model or homogeneous solid diffusion model) for determining adsorbate-adsorbent diffusion coefficients.

$$\frac{m_t}{m_\infty} = 1 - \frac{6}{\pi^2}\sum \frac{1}{n^2}\exp\left(-\frac{n^2\pi^2 D_c\, t}{r_c^2}\right) \qquad (1)$$

where m_t is the amount of adsorbate (g) adsorbed at time t, m_∞ is the amount of adsorbate (g) adsorbed after lapse of infinite time (when the adsorbents were saturated with adsorbate), D_c is the diffusion coefficient ($m^2.s^{-1}$), r_c is the radius of adsorbent particles (m), and t is the lapse of time (s). In Equation (1), D_c is assumed to be independent of adsorbate concentration, and adsorbents are supposed as approximately spherical particles [47]. Experimental kinetic data of benzene and ethylbenzene adsorption were also compared with pseudo-first-order and pseudo-second-order models of adsorption of gases. Before the experiments, each sample was degassed at 120 ºC for 4 h. All the experiments were replicated with three adsorbents for two pollutants (benzene and ethylbenzene) at room temperature.

2.4. Adsorption kinetic

Adsorption and desorption kinetics are significant in actual processes [6] and are studied for an investigation of a rate-controlling step. The rate-controlling step relies upon the adsorbent, adsorbate, and solution specifications. Generally, important factors in the adsorption process are adsorbent particle size, adsorbate concentration, mixing quality, interaction between adsorbate and adsorbent, and adsorbate diffusion coefficients [52]. Intra-particle diffusion is the rate-controlling step of adsorption in processes containing adsorbent with large particle size, the high concentration of adsorbate, and low adsorbent-adsorbate interaction [52]. In physisorption processes, linear driving force (LDF) interprets intra-particle mass transfer [52]. The pseudo-first-order model (linear driving force model) is used for the prediction of adsorption kinetics of several gases or vapors on activated carbons, crystalline compounds, carbon molecular sieves, and silica mesoporous materials such as silica aerogel [6]. The LDF model pertaining to the adsorption rate is described by the following equation:

$$q_t = q_e(1 - e^{-k_f t}) \qquad (2)$$

where q_e ($mmol.g^{-1}$) and q_t ($mmol.g^{-1}$) represent the amounts of benzene and ethylbenzene adsorbed at equilibrium and at a given point of time, respectively. k_f (s^{-1}) is the first-order rate constant [43]. According to the point of view of the second-order kinetic model, the rate-controlling step is chemical interactions such as strong covalent bonding between gas and adsorbent surface [44, 52]. This model is given by the following expression:

$$q_t = \frac{q_e^{\,2} k_s t}{1 + q_e k_s t} \qquad (3)$$

where k_s ($g.mmol^{-1}s^{-1}$) is the second-order rate constant [44].

The validity of the fit of experimental data with kinetic models was approximated by the following error function:

$$\Delta q(\%) = \sqrt{\frac{\sum[\frac{q_{exp} - q_{model}}{q_{exp}}]^2}{N - 1}} * 100 \qquad (4)$$

where $\Delta q(\%)$ is the normalized standard deviation, q_{exp} and q_{model} are the experimental and theoretical amounts of benzene and ethylbenzene adsorbed, and N is the number of data in each isotherm [44].

3. Results and discussion

3.1. Properties of synthesized samples

The structural properties of synthesized samples are listed in Table 1. This table shows that the synthesized samples are nanostructured and mesoporous (2-50 nm). As shown in Table 1, the addition of activated carbon in the silica aerogel matrix leads to the decrease of specific surface area and increase of average pores diameter, density, and volume of total pores. The specific surface area of pure silica aerogel is greater than that of silica aerogel-activated carbon composites. Specific surface area has a reverse relationship with density and pore size distribution. Hence, pure silica aerogel has the greatest specific surface area. Silica aerogel-activated carbon composite has higher density than pure silica aerogel, and this property increases with the addition of activated carbon in the silica aerogel matrix, because the density of activated carbon is higher than that of pure silica aerogel.

Table 1
Structural properties of synthesized adsorbents.

Adsorbent	B.E.T. surface area (m^2g^{-1})	Average pores diameter (nm)	Volume of total pores (cm^3g^{-1})	Density (gcm^{-3})
Silica aerogel	427.16	19.72	2.11	0.16
Silica aerogel-2 % wt activated carbon composite	358.4	29.51	2.64	0.22
Silica aerogel-0.5 % wt activated carbon composite	360.1	32.38	2.91	0.18

Figures 1 and 2 show SEM images and the pore size distribution (PSD) profiles of the silica aerogel and silica aerogel-activated carbon composites synthesized by an ambient pressure drying (APD) method, respectively. Figure 1 exhibits the porous network structure, which contains spherical solid clusters, pores below 100 nm, and the uniform particle distribution of samples. The particles size of composites is greater than that of pure silica aerogel. Therefore, it can be mentioned that the surface modification reaction in the composites is completely done.

A noticeable change has been observed in the PSD profiles of the silica aerogel and silica aerogel-activated carbon composites. Based on Figure 2, it is known that synthesized samples contain mesopores (2–50 nm pores) and macropores (above 50 nm). Most pores of silica aerogel were mesopores (below 20 nm), and the peak of its smallest pore was 8nm, whereas most pores of silica aerogel composites were mesopores (below about 30 nm) and the peak of their smallest pore was 16 nm.

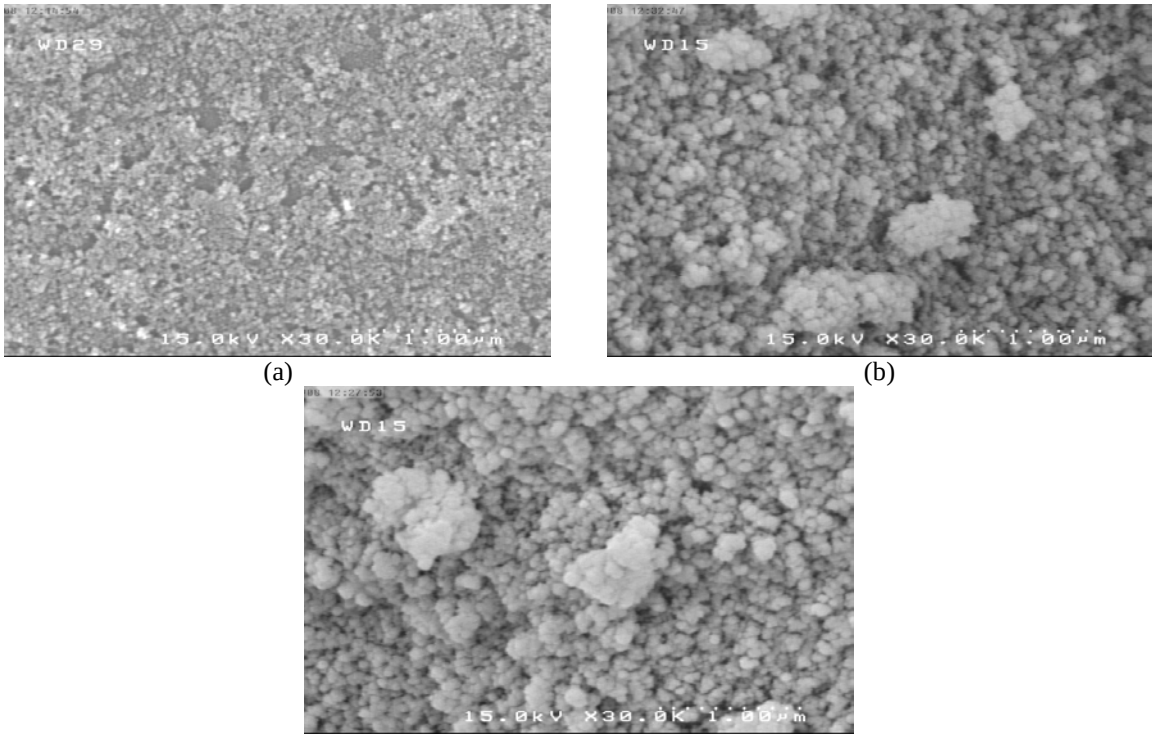

Figure 1. SEM images of (a) silica aerogel, (b) silica aerogel-0.5 % wt activated carbon composite, and (c) silica aerogel-2 % wt activated carbon composite.

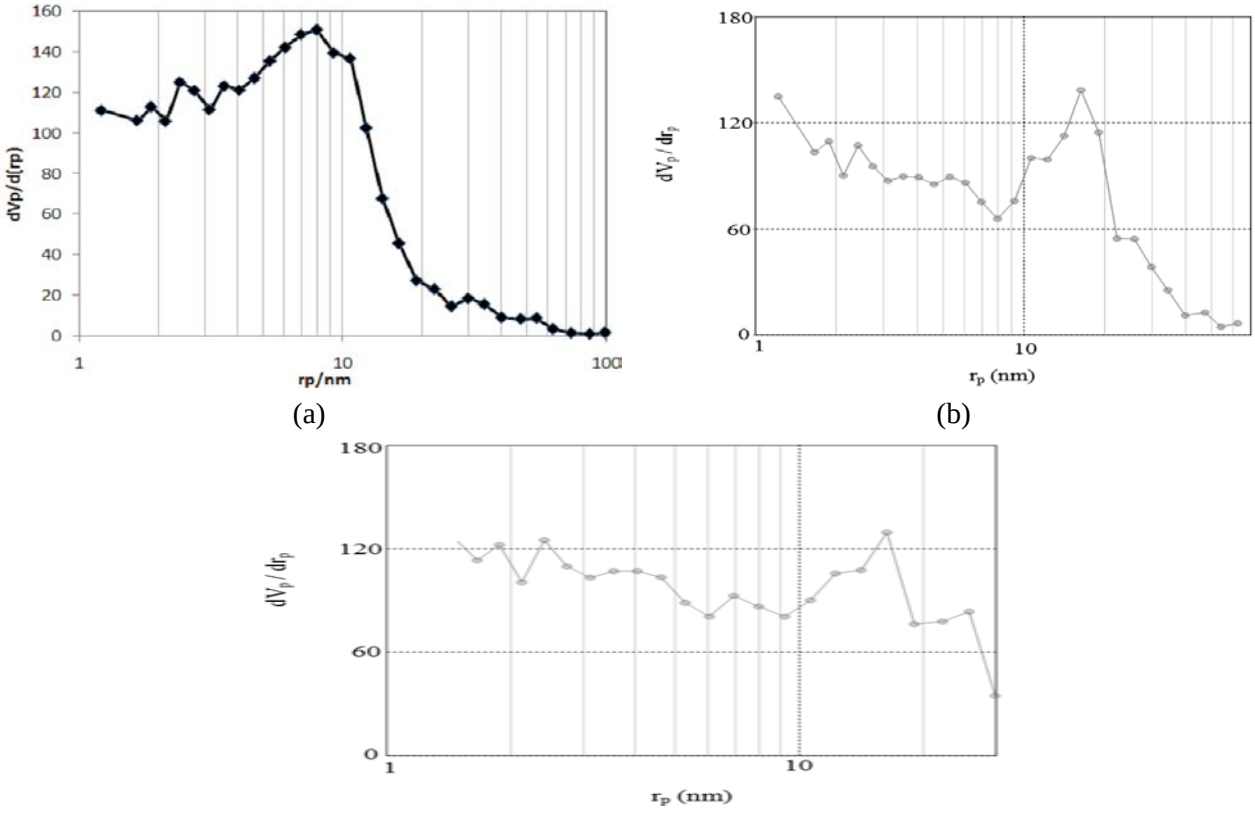

Figure 2. Pore size distribution of the water glass based (a) silica aerogel, (b) silica aerogel-0.5 % wt activated carbon composite, and (c) silica aerogel-2 % wt activated carbon composite dried at an ambient pressure.

In surface modification reaction, -Si−$(OH)_3$ groups are replaced with nonpolar stable -Si−$(CH_3)_3$ groups. Because of the existence of a repulsive force between -Si−$(CH_3)_3$ groups, the volume of gels increases (''spring back'' phenomenon), and pores of gels become greater [53]. The average pore diameter of composites is greater than that of pure silica aerogel. Therefore, surface modification reaction in the samples containing activated carbon is completely done, and the number of -Si−$(CH_3)_3$ groups in composite is more than that of pure silica aerogel. The FTIR analysis shows this fact too. Figure 3 shows the FTIR analysis of synthesized samples. This figure represents that the peaks of 3500 cm^{-1} and 1600 cm^{-1}correspond to the O–H groups. The peaks at around 1100 and 800 cm^{-1} are due to SiO_2 groups [6, 53]. The absorption peaks of $-CH_3$ at 846, 1256, and 2963 cm^{-1} are related to the surface modification agent of TMCS [54].

Based on this figure, the intensity of O–H peak in synthesized samples changes in order of silica aerogel> silica aerogel-0.5 % wt activated carbon composite > silica aerogel-2 % wt activated carbon composite. Thus, surface modification reaction in the silica aerogel-activated carbon composites was completely done, and the hydrophobicity of composites increased with an increment of activated carbon in the silica aerogel matrix.

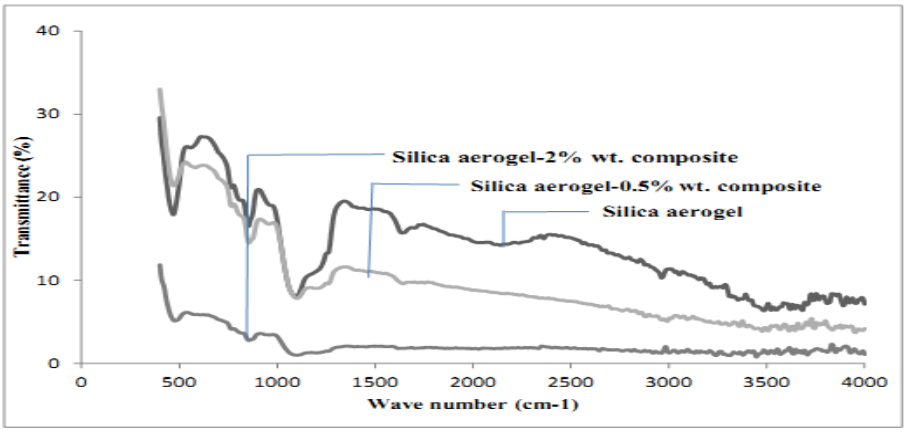

Figure 3. FTIR spectra of synthesized samples.

3.2. Adsorption isotherms

Figures 4 and 5 show the adsorption isotherms (increment of adsorbent weight with lapse of time) of benzene and ethylbenzene over silica aerogel, silica aerogel- 2 % wt activated carbon composite, and silica aerogel- 0.5 % wt activated carbon composite at three adsorbent weights of 0.01, 0.02, and 0.04 g, respectively. It is evident that the saturation time of adsorbents and amount of adsorbate increase with an increment of the amount (weight) of used adsorbent; however, equilibrium adsorption capacity (adsorbate (mg)/adsorbent (g)) decreases approximately (also, see Tables 4 and 5). The adsorption process is proportional to the total pore volume of adsorbent and available surface area for adsorbate. Therefore, by increasing the amount of used adsorbent, the saturation time and amount of adsorbate increase. The decrease of equilibrium adsorption capacity depends on the diffusion phenomenon and the rate-controlling step.

The effect of these phenomena is presented at the end of this part and the next part (Comparison of Kinetic Models).

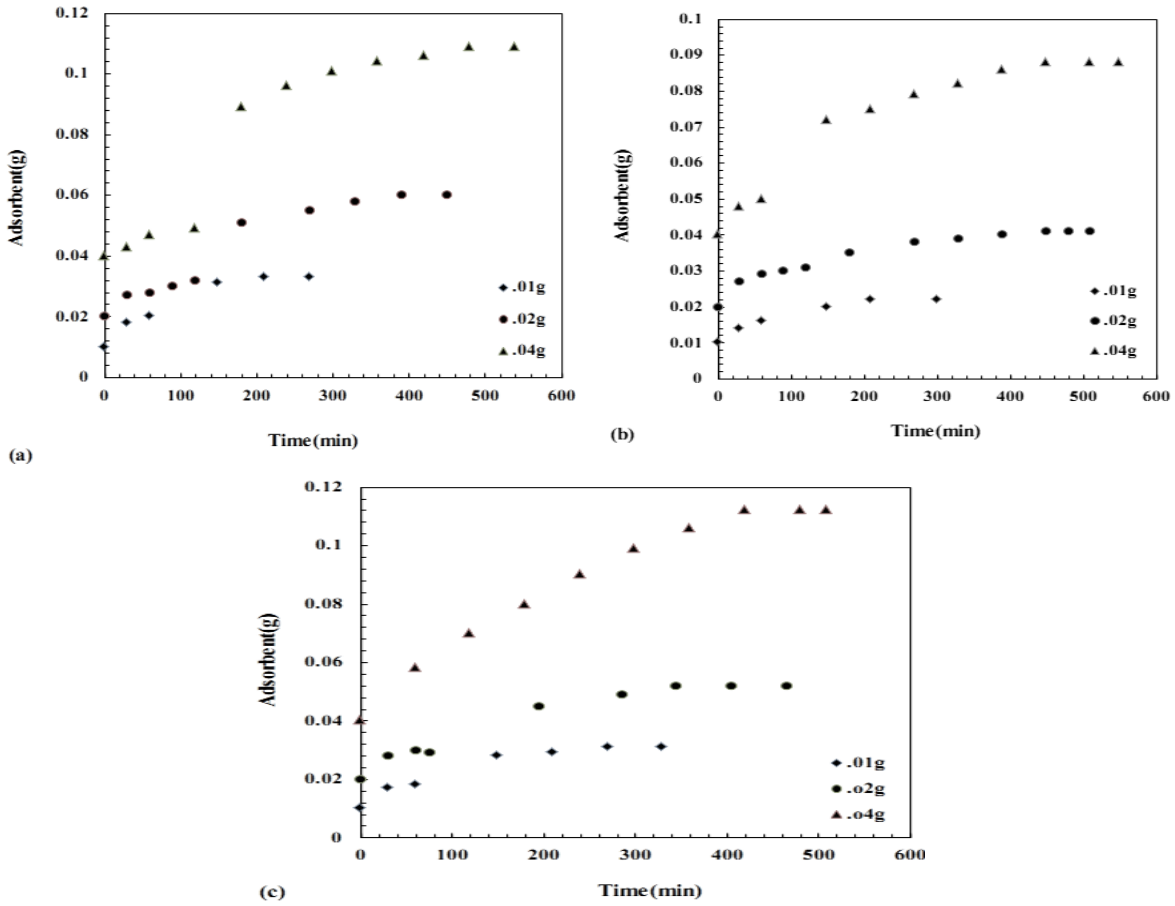

Figure 4. Benzene adsorption isotherms over (a) silica aerogel, (b) silica aerogel-0.5 % wt activated carbon composite, and (c) silica aerogel-2 % wt activated carbon composite at three adsorbent weights of 0.01, 0.02, and 0.04 g.

The results also show that the amount of ethylbenzene adsorption over silica aerogel and its composites is less than that of benzene. The presence of alkyl bond in the ethylbenzene structure causes that ethylbenzene diffusion and adsorption over silica aerogel and its composites becomes limited. Also, there is a limited interaction between adsorbent and adsorbate because of the existence of alkyl bond in ethylbenzene and methyl bond in silica aerogel and its composites, resulting in the reduction of ethylbenzene adsorption. According to Figure 5, it can also be observed that, in ethylbenzene adsorption, in spite of other trends, the saturation time of high-quantity silica aerogel-0.5 % wt activated carbon composite (0.04 g) is less than that of low-quantity silica aerogel-0.5 % wt activated carbon composite (0.01 and 0.02 g). This inconsistency is associated with non-uniformity of synthesized adsorbents and different adsorbents of major sizes. These facts result in major diffusion coefficient of ethylbenzene for adsorbent with high-quantity and cause the reduction of saturation time. In the ideal adsorption process and in constant operational conditions, the equilibrium adsorption capacity of adsorbents must be the same at different weight quantities of adsorbents, because the equilibrium adsorption capacity is one of the adsorbent characteristics. However, in this work, equilibrium adsorption capacity has changed by changing adsorbent quantity in the constant conditions of the experiment. The

reasons of this change are associated with the distribution of adsorbent particles, different sizes, and accumulation of adsorbent particles in the experimental container, limiting the access of adsorbate molecules to adsorbents and leading to the reduction of diffusion coefficient and equilibrium adsorption capacity. Therefore, in high-scale adsorption processes (semi-industrial and industrial), the amount of adsorbent must be optimized, and the conditions and equipment of the process should be adjusted until all of adsorbent particles become accessible for adsorbate. The results show that silica aerogel has the highest adsorption capacity of benzene and ethylbenzene vapors. Also, a comparison of molecular size of benzene and ethylbenzene (2.798 nm and 5.318 nm, respectively) and the pore size of synthesized aerogels (see table 1) shows that silica aerogels and silica aerogel-activated carbon composites are suitable adsorbents for adsorption of volatile organic compounds, especially benzene and ethylbenzene.

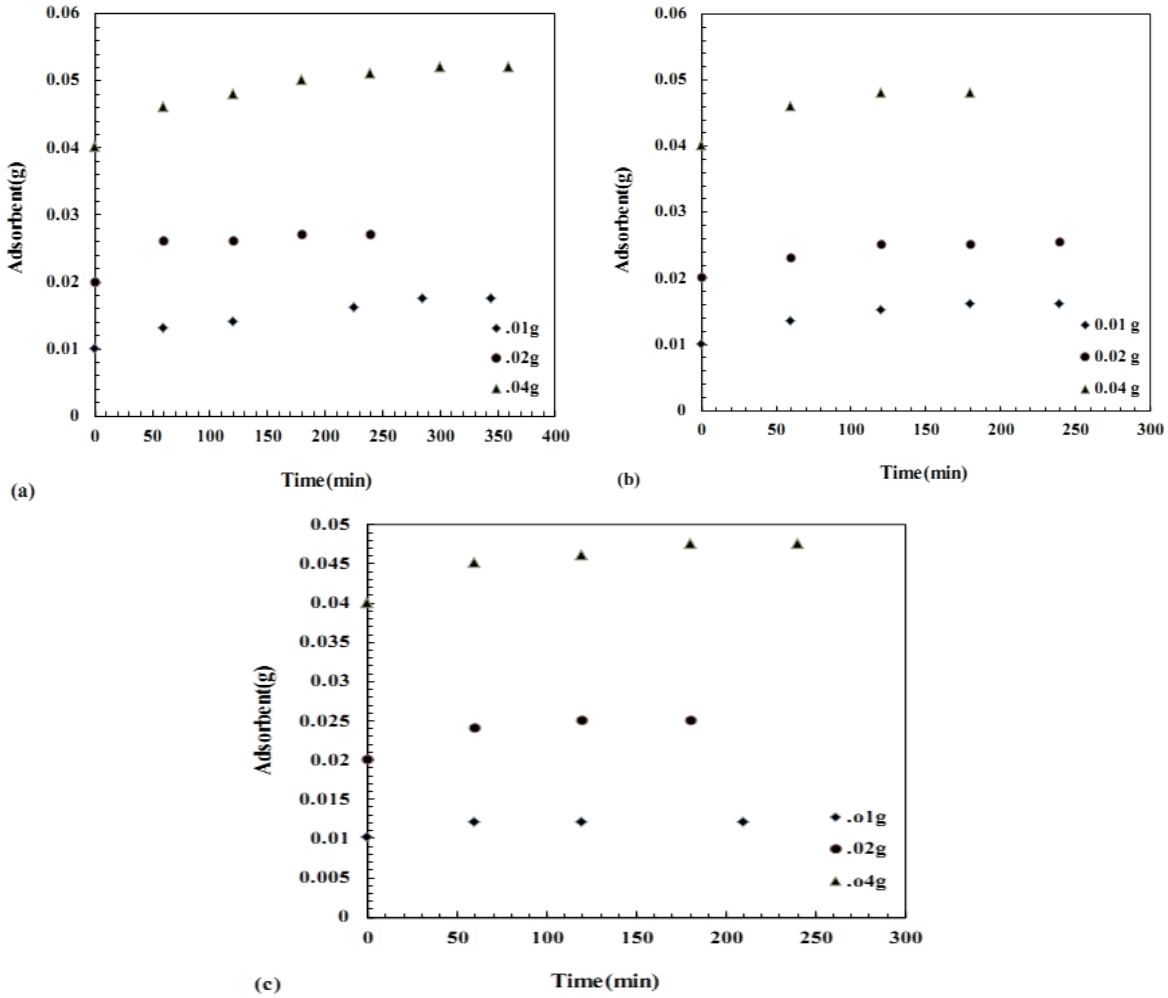

Figure 5. Ethyl benzene adsorption isotherms over (a) silica aerogel, (b) silica aerogel-0.5 % wt activated carbon composite, and (c) silica aerogel-2 % wt activated carbon composite at three adsorbent weights of 0.01, 0.02, and 0.04 g.

3.3. Comparison of kinetic models

Figures 6 and 7 show the amount of adsorbate versus time and the corresponding profiles predicted by pseudo-first- and pseudo-second-order models for benzene and ethylbenzene adsorption over silica aerogel- and silica

aerogel-activated carbon composites, respectively. Generally, the adsorption process consists of four sequential steps: (i) the adsorbate transfers from the bulk to the external film around the adsorbents; (ii) the adsorbate overcomes the external film resistance and transfers across the boundary layer; (iii) the adsorbate overcomes micropore resistance and diffuses into the pores; (iv) adsorption and desorption between the adsorbate and active sites. The entire process may be controlled by one of the mentioned steps, or by a combination of them [52].

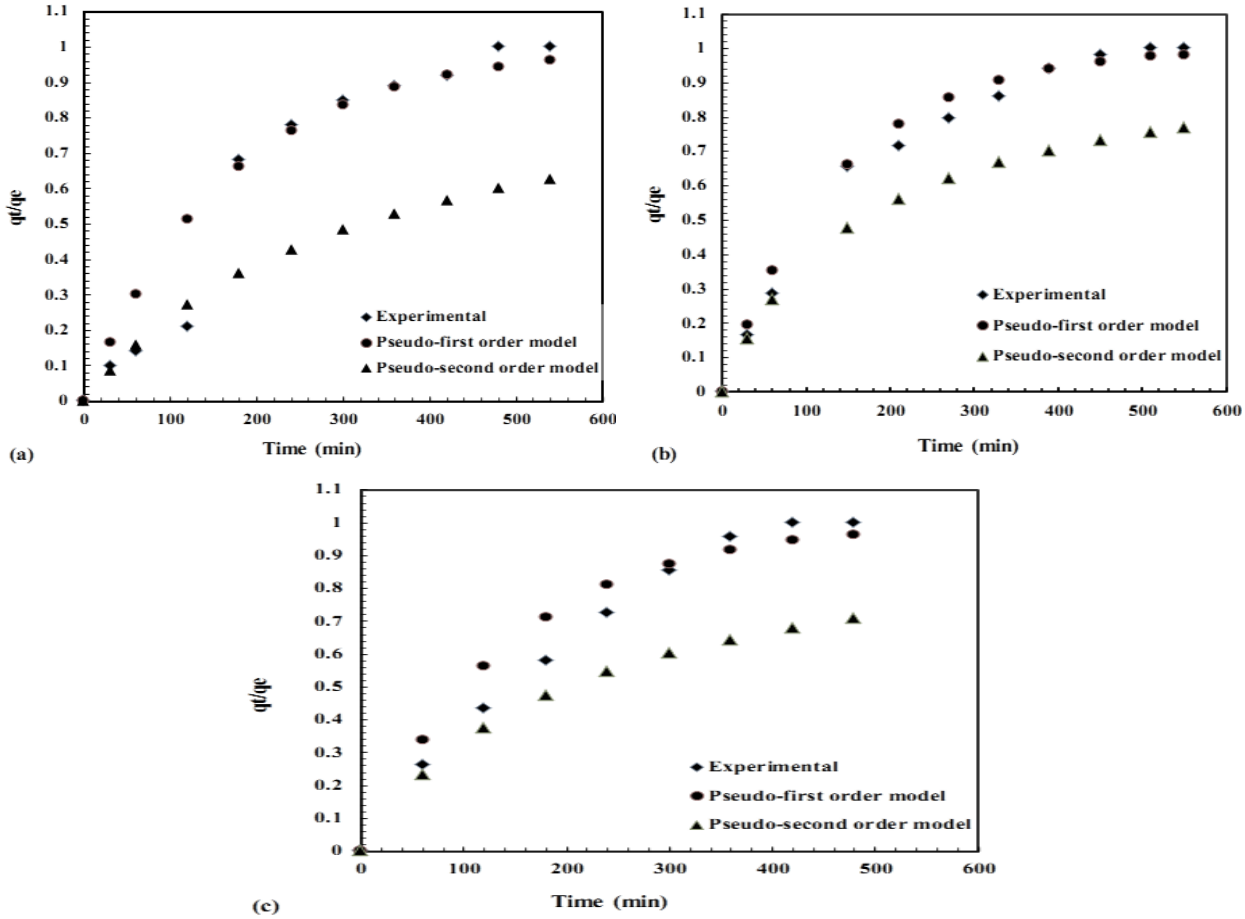

Figure 6. Pseudo-first-order and pseudo-second-order fits for benzene adsorption over (a) silica aerogel, (b) silica aerogel-0.5 % wt activated carbon composite, and (c) silica aerogel-2 % wt activated carbon composite.

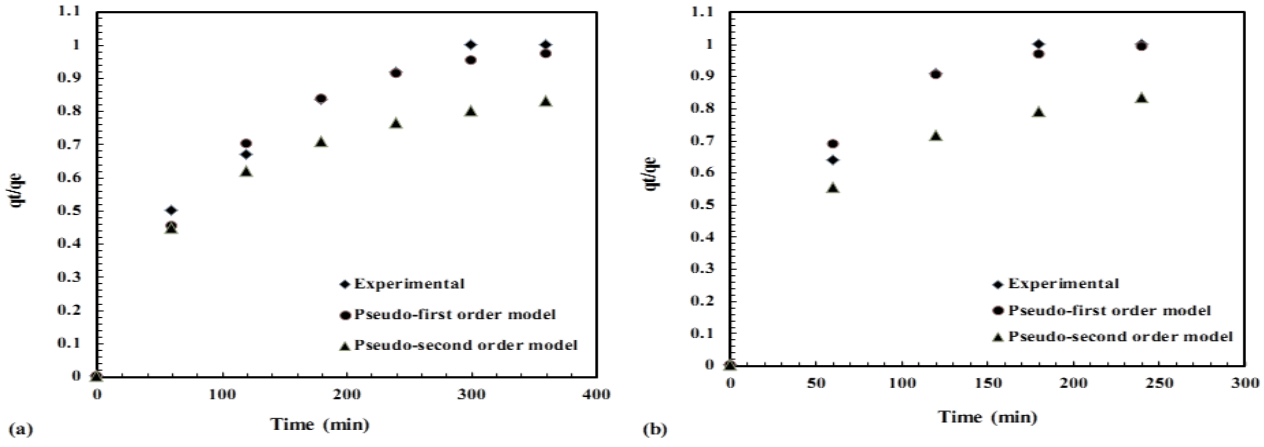

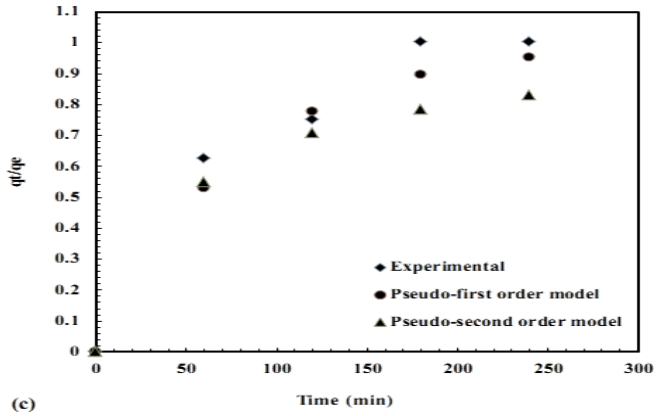

Figure 7. Pseudo-first-order and pseudo-second-order models fit for ethylbenzene adsorption over (a) silica aerogel, (b) silica aerogel-0.5 % wt activated carbon composite, and (c) silica aerogel-2 % wt activated carbon composite.

Based on Figures 6 and 7, it is evident that adsorption kinetics of benzene and ethylbenzene over silica aerogel and silica aerogel-activated carbon composites follow the pseudo-first-order model, approximately. So, in benzene and ethylbenzene adsorption over silica aerogel and its composites, diffusion through porosity with a size similar to that of adsorbate or surface diffusion barrier is the rate-controlling step. Based on Table 2, it can be observed that the deviation of experimental q values from q values calculated by the pseudo-first-order model for benzene adsorption over silica aerogel and silica aerogel-2 % wt activated carbon composite is more than those calculated by the pseudo-second-order model. Because the adsorption mechanism works differently at the beginning of the adsorption process and the rate-controlling step is chemical interactions leading to binding of gas to the adsorbent surface by strong covalent bonding. Therefore, the pseudo-second-order model must be applied to modeling the beginning of the silica aerogel and silica aerogel-2 % wt activated carbon composite adsorption. The kinetic parameters provide information about designing and modeling the adsorption process. These parameters are determined for pseudo-first-order and pseudo-second-order models by nonlinear regression.

Table 2
Accuracy of the fit of the kinetic models.

Adsorbate	Adsorbent	Pseudo-first-order model, Δq_f (%)	Pseudo-second-order model, Δq_s (%)
Benzene	Silica aerogel	63	36
	Silica aerogel-2 % wt activated carbon composite	55	34
	Silica aerogel-0.5 % wt sctivated carbon composite	10	21
Ethyl benzene	Silica aerogel	4	15
	Silica aerogel-2 % wt activated carbon composite	9	15
	Silica aerogel-0.5 % wt activated carbon composite	4	18

According to Table 3, the pseudo-first-order and -second-order model parameters of ethylbenzene are greater than those of benzene. Because the molecular weight of ethylbenzene is larger than that of benzene and quickly moves from the bulk solution to the boundary layer surrounding the adsorbent particles. Also, the interaction between ethyl group of ethylbenzene structure and functional groups of silica aerogel and its composites leads to major parameters (k_f and k_s) for ethylbenzene adsorption kinetic. It is evident that the saturation time of ethylbenzene adsorption is less than that of benzene adsorption because of the major adsorption rate constant of ethylbenzene. As shown in Table 3, benzene and ethylbenzene have the greatest adsorption rate constant over silica aerogel- 0.5 % wt activated carbon composite. Because silica aerogel- 0.5 % wt activated carbon composite has the greatest average pore diameter.

Table 3
Adsorption rate constants.

Adsorbate	Adsorbent	First-order rate constant, k_f (s^{-1})	Second-order rate constant, k_s (g $mmol^{-1}s^{-1}$)
Benzene	Silica aerogel	0.007	0.00014
	Silica aerogel-2 % wt activated carbon composite	0.005	0.00023
	Silica aerogel-0.5 % wt activated carbon composite	0.007	0.00039
Ethyl benzene	Silica aerogel	0.01	0.0048
	Silica aerogel-2 % wt activated carbon composite	0.012	0.0107
	Silica aerogel-0.5 % wt activated carbon composite	0.014	0.0160

3.4. Diffusion coefficient of benzene and ethylbenzene

Tables 4 and 5 list the diffusion coefficients, saturation time, and equilibrium adsorption capacity for benzene and ethylbenzene, respectively. It is evident that benzene and ethylbenzene diffusion coefficient in adsorbents changes in order of silica aerogel- 0.5 % wt activated carbon composite> silica aerogel- 2 % wt activated carbon composite> silica aerogel. This result can be explained by the procedure of changing of adsorbent pores average diameter. The pore average diameter of adsorbents changes in the order of silica aerogel- 0.5 % wt activated carbon composite> silica aerogel- 2 % wt activated carbon composite> silica aerogel. Therefore, the procedure of changing diffusion coefficient is the same as that of the pore average diameter. In addition, the diffusion coefficient can be directly related to the adsorption kinetic since the procedure of changing benzene diffusion coefficient approximately matches the procedure of benzene adsorption kinetic.

Therefore, diffusion coefficient depends on both adsorbent structure and adsorption kinetic. The description of equilibrium adsorption capacity and saturation time of adsorbents is presented in the Adsorption Isotherms section. It can be observed from Tables 4 and 5 that diffusion coefficient

decreases with an increment of the amount of adsorbent. By increasing the amount of adsorbent, adsorbent particles accumulate on each other and diffusion resistance increases; thus, the diffusion coefficient decreases. Also, it is evident that diffusion coefficient of ethylbenzene is greater than that of benzene.

Table 4
Saturation time of adsorbent, equilibrium adsorption capacity, and diffusion coefficient for benzene.

Adsorbent with different weights (g)		Saturation time (min)	Amount of adsorbate (mg)	Equilibrium adsorption capacity (mg g^{-1})	Diffusion coefficient (m^2 s^{-1})
Silica aerogel	0.01	210	23	2300	2.6 E-13
	0.02	390	40	2000	7.11 E-14– 6.66 E-13
	0.04	480	72	1800	2.16 E-14– 5.64 E-13
Silica aerogel-2 % wt activated carbon composite	0.01	270	21	2100	5.64 E-12
	0.02	345	32	1600	3.55 E-12
	0.04	420	69	1725	8.5 E-13–2.86 E-12
Silica aerogel-0.5 % wt activated carbon composite	0.01	210	12	1200	5.58 E-12–1.4 E-11
	0.02	450	21	1050	5.8 E-12–1.1 E-11
	0.04	510	49	1225	5.54 E-12–1.27 E-11

Table 5
Saturation time of adsorbent, equilibrium adsorption capacity, and diffusion coefficient for ethyl benzene.

Adsorbent with different weights (g)		Saturation time (min)	Amount of adsorbate (mg)	Equilibrium adsorption capacity (mg g^{-1})	Diffusion coefficient (m^2 s^{-1})
Silica aerogel	0.01	285	7	700	3.65 E-13
	0.02	180	7.5	375	1.95 E-12– 9.78 E-13
	0.04	300	12	300	6.26 E-13
Silica aerogel-2 % wt activated carbon composite	0.01	120	2.5	250	1.78 E-11
	0.02	120	5	250	1.76 E-11
	0.04	180	8	200	7.34 E-12
Silica aerogel-0.5 % wt activated carbon composite	0.01	120	5	500	1.98 E-11
	0.02	180	6	300	5.5 E-12–1.82 E-11
	0.04	120	8	200	2.5 E-12

Adsorption of benzene on silica aerogel and its composites is of a mono layer, and adsorbate molecules are often adsorbed on active sites of adsorbent surface. However, in the absorption of ethylbenzene, due to the poor interaction between the ethyl branch and the functional groups in the adsorbent structure, absorbate molecules are absorbed through diffusion into absorbent pores. Also, considering the high adsorption capacity of benzene compared to ethyl benzene, it can be said that the rate-limiting step of the adsorption process in the adsorption of benzene and ethylbenzene is the diffusion into the pores step and the adsorbate transport from the bulk to the external film around the

adsorbents step, respectively. Therefore, according to the above, it can be said that diffusion coefficient of benzene is lower than that of ethylbenzene. Table 6 shows the comparison between calculated diffusion coefficients and diffusion coefficients determined by other researchers. It is evident that there is no significant deviation between diffusion coefficients determined in this work and those in other references. Therefore, for determining the diffusion coefficient of benzene and ethylbenzene in silica aerogel and its composites, the intra-particle diffusion model or homogeneous solid diffusion model (Equation (1)) can be used effectively.

Table 6
Comparison of diffusion coefficients determined in this study and diffusion coefficients presented in the selected literature.

Adsorbent	Adsorbate	Diffusion coefficient D (m^2 s^{-1})	Reference
Bentonite (2 % activated carbon)	Benzene	3 E-10	[55]
Bentonite (10 % activated carbon)		4 E-10	
Bentonite (no activated carbon)		3 E-10	
Bentonite (2 % activated carbon)	Toluene	3 E-10	
Bentonite (10 % activated carbon)		4 E-10	
Bentonite (no activated carbon)		3 E-10	
Building materials	VOC	7.65 E-11	[56]
Activated carbon	Toluene	5 E-10–5 E-9	[48]
Cement	Ethyl benzene	0.67 E-10–3.05 E-10	[57]
Zeolite crystals	Adsorption of gases and vapours	1 E-15–1 E-13	[47]
Silica aerogel	Benzene	3.17 E-13	This article
Silica aerogel-2 % wt activated carbon composite		3.2 E-12	
Silica aerogel-0.5 % wt activated carbon composite		9.1 E-12	
Silica aerogel	Ethyl benzene	9.79 E-13	
Silica aerogel-2 % wt activated carbon composite		1.42 E-11	
Silica aerogel-0.5 % wt activated carbon composite		1.7 E-11	

4. Conclusions

In this study, silica aerogel and silica aerogel-activated carbon composites were synthesized using a water glass precursor via two-step sol-gel method followed by ambient pressure drying. In order to surface modification of the resultant samples, hydrophilic $-OH$ groups were replaced with hydrophobic $-CH_3$ groups using surface modification reagent (TMCS). The synthesized samples exhibited mesoporous structures with an average pore size of 8 and 16 nm for silica aerogel and silica aerogel-activated carbon composites, respectively. After synthesis, benzene and

ethylbenzene adsorption over silica aerogel and silica aerogel-activated carbon composites were studied at three weights of 0.01, 0.02, and 0.04 g for an investigation of equilibrium adsorption capacity, saturation time of adsorbent, kinetics of adsorption, and diffusion coefficient. Obtained results showed that by increasing the amount of adsorbent, the saturation time increased; however, equilibrium adsorption capacity decreased. Ethylbenzene adsorption capacity of synthesized adsorbents was less than that of benzene adsorption capacity. Silica aerogel has the maximum adsorption capacity of benzene (2033 $mg.g^{-1}$) and ethylbenzene (458 $mg.g^{-1}$). The equilibrium adsorption capacity of benzene on silica aerogel-2 % wt activated carbon composite (1808 $mg.g^{-1}$) is more than that of silica aerogel-0.5 % wt activated carbon composite (1158 $mg.g^{-1}$). Static adsorption results showed that silica aerogel and its composites had good affinity towards aromatic molecules, especially benzene, fast adsorption kinetics due to their superior adsorption capacity, and faster diffusion process. Pseudo-first-order kinetic model approximately describes the adsorption kinetic of benzene and ethylbenzene on silica aerogel and its composites, suggesting that the adsorption process is controlled by physisorption. The pseudo-second-order model describes the beginning of the benzene adsorption kinetic on silica aerogel and silica aerogel-2 % wt activated carbon composite, suggesting that the rate-controlling step is chemical interactions such as strong covalent bonding. Diffusion of benzene and ethylbenzene within the silica aerogel-0.5 % wt activated carbon composite has the maximum diffusivity of $9.12 \times^{-12}$ and $1.15 \times^{-12}$ $m^2.s^{-1}$, respectively.

Nomenclature

m	mass [g].
v	volume [cm^{-3}].
D_c	diffusion coefficient [m^2s^{-1}].
r_c	radius of adsorbent particles [m].
k_f	First-order rate constant [s^{-1}].
k_s	second-order rate constant [$gmmol^{-1}s^{-1}$].
q_e	amount of benzene and ethyl benzene adsorbed at equilibrium [$mmolg^{-1}$].
q_t	amount of benzene and ethyl benzene adsorbed at a given point of time [$mmolg^{-1}$].
Δq	normalized standard deviation.

Greek letters

ρ	density [gcm^{-3}].

Abbreviations

VOC	volatile organic compound.
BTEX	benzene, toluene, ethyl benzene, xylene.
HSDM	homogeneous solid diffusion model.
TMCS	trimethylchlorosilane.
IPA	isopropyl alcohol.
SEM	scanning electron microscopy.
BET	brunauer–emmitt–teller.
FTIR	fourier transform infrared spectroscopy.
LDF	linear driving force.
PSD	pore size distribution.
APD	ambient pressure drying.

Acknowledgement

The authors would like to thank Sahand University of Technology and Iran Nanotechnology Initiative Council for financial supports.

References

[1] Campesi, M. A., Luzi, C. D., Barreto, G. F. and Martínez, O. M., "Evaluation of an adsorption system to concentrate VOC in air streams prior to catalytic incineration", *J. Environ. Manage.*, **154**,

216 (2015).

[2] Hosseini, M., Barakat, T., Cousin, R., Aboukaïs, A., Su, B. and De, W. G., "Catalytic performance of core–shell and alloy Pd–Au nanoparticles for total oxidation of VOC: The effect of metal deposition", *Appl. Catal.*, **111–112**, 218 (2012).

[3] Hsu, S. H., Huang, C. S., Chung, T. W. and Gao, S., "Adsorption of chlorinated volatile organic compounds using activated carbon made from Jatropha curcas seeds", *J. Taiwan Inst. Chem. Eng.*, **45**, 2526 (2014).

[4] Tamaddoni, M., Sotudeh-Gharebagh, R., Nario, S., Hajihosseinzadeh, M. and Mostoufi, N., "Experimental study of the VOC emitted from crude oil tankers", *Process Saf. Environ. Prot.*, **92**, 929 (2014).

[5] Vinodh, R., Jung, E. M., Ganesh, M., Peng, M. M., Abidov, A., Palanichamy, M., Cha, W. S. and Jang, H. T., "Novel microporous hypercross-linked polymers as sorbent for volatile organic compounds and CO_2 adsorption", *J. Ind. Eng.*, **21**, 1231 (2015).

[6] Dou, B., Li, J., Wang, Y., Wang, H., Ma, C. and Hao, Z., "Adsorption and desorption performance of benzene over hierarchically structured carbon–silica aerogel composites", *J. Hazard. Mater.*, **196**, 194 (2011).

[7] William, J. C. and Lead, P. E., VOC control strategies in plant design, in Chemical processing: Project engineering annual, p. 44 (1997).

[8] Zhao, Z., Li, X. and Li, Z., "Adsorption equilibrium and kinetics of p-xylene on chromium-based metal organic framework MIL-101", *Chem. Eng. J.*, **173**, 150 (2011).

[9] Zaitan, H., Bianchi, D., Achak, O. and Chafik, T., "A comparative study of the adsorption and desorption of o-xylene onto bentonite clay and alumina", *J. Hazard. Mater.*, **153**, 852 (2008).

[10] Anfruns, A., Martin, M. and Montes-Morán, M. A., "Removal of odourous VOCs using sludge-based adsorbents", *Chem. Eng. J.*, **166**, 1022 (2011).

[11] Blanco, F., Vilanova, X., Fierro, V., Celzard, A., Ivanov, P., Llobet, E., Canellas, N., Ramırez, J. L. and Correig, X., "Fabrication and characterisation of microporous activated carbon-based pre-concentrators for benzene vapours", *Sens Actuators*, **132** (B), 90 (2008).

[12] Hung, C., Bai, H. and Karthik, M., "Ordered mesoporous silica particles and Si MCM-41 for the adsorption of acetone: A comparative study", *Sep. Purif. Technol.*, **64**, 265 (2009).

[13] Romero-Anaya, A. J., Romero-Anaya, M. A. and Linares-Solano, A., "Factors governing the adsorption of ethanol on spherical activated carbons", *Carbon*, **83**, 240 (2015).

[14] Horikawa, T., Sakao, N. and Do, D. D., "Effects of temperature on water adsorption on controlled microporous and mesoporous carbonaceous solids", *Carbon*, **56**, 183 (2013).

[15] Kim, K. D., Park, E. J., Seo, H. O., Jeong, M. G., Kim, Y. D. and Lim, D. C., "Effect of thin hydrophobic films for toluene adsorption and desorption behaviour on activated carbon fiber under dry and humid conditions", *Chem. Eng. J.*, **200**, 133 (2012).

[16] Bandura, L., Franus, M., Józefaciuk, G. and Franus, W., "Synthetic zeolites from fly ash as effective mineral sorbents for land-based petroleum spills cleanup",

Fuel, **147**, 100 (2015).

[17] Qu, F., Zhu, L. and Yang, K., "Adsorption behaviors of volatile organic compounds (VOCs) on porous clay heterostructures (PCH)", *J. Hazard. Mater.*, **170**, 7 (2009).

[18] Dıaz, E., Ordonez, S., Vega, A. and Coca, J., "Adsorption characterisation of different volatile organic compounds over alumina, zeolites and activated carbon using inverse gas chromatography", *J. Chromatogr. A*, **1049**, 139 (2004).

[19] Dou, B., Hu, Q., Li, J., Qiao, S. and Hao, Z., "Adsorption performance of VOCs in ordered mesoporous silicas with different pore structures and surface chemistry", *J. Hazard. Mater.*, **186**, 1615 (2011).

[20] Duerinck, T., Leflaive, P., Arik, I. C., Pirngruber, G., Meynen, V., Cool, P., Martens, J. A., Baron, G. V., Faraj, A. and Denayer, J. F. M., "Experimental and statistical modeling study of low coverage gas adsorption of light alkanes on meso-microporous silica", *Chem. Eng. J.*, **179**, 52 (2012).

[21] Russo, P. A., Ribeiro, M. M. L. and Carrott, P. J. M., "Trends in the condensation/evaporation and adsorption enthalpies of volatile organic compounds on mesoporous silica materials", *Microporous Mesoporous Mater.*, **51**, 223 (2012).

[22] Gallego, E., Roca, F. J., Perales, J. F. and Guardino, X., "Experimental evaluation of VOC removal efficiency of a coconut shell activated carbon filter for indoor air quality enhancement", *Buil. Env.*, **67**, 14 (2013).

[23] Sarawade, P. B., Kim, J. K., Hilonga, A., Quang, D. V., Jeon, S. J. and Kim, H. T., "Synthesis of sodium silicate-based hydrophilic silica aerogel beads with superior properties: Effect of heat-treatment", *J. Non-Cryst. Solids*, **357**, 2156 (2012).

[24] Omranpour, H. and Motahari, S., "Effects of processing conditions on silica aerogel during aging: Role of solvent, time and temperature", *J. Non-Cryst. Solids*, **379**, 7 (2013).

[25] Sarawade, P. B., Kim, J. K., Hilonga, A. and Kim, H. T., "Production of low-density sodium silicate-base d hydrophobic silica aerogel beads by a novel fast gelation process and ambient pressure drying process", *Solid State Sci.*, **12**, 911 (2010).

[26] Yang, H., Ye, F., Liu, Q., Liu, S., Gao, Y. and Liu, L., "A novel silica aerogel/porous Si_3N_4 composite prepared by freeze casting and sol-gel impregnation with high-performance thermal insulation and wave-transparent", *Mater. Lett.*, **138**, 135 (2015).

[27] Attia, S. M., Sharshar, T., Abd-Elwahed, A. R. and Tawfik, A., "Study of transport properties and conduction mechanism of pure and composite resorcinol formaldehyde aerogel doped with Co-ferrite", *Mater. Sci. Eng.*, **178**, 897 (2013).

[28] Alnaief, M. and Smirnova, I., "Effect of surface functionalization of silica aerogel on their adsorptive and release properties", *J. Non-Cryst. Solids*, **365**, 1644 (2010).

[29] Meynen, V., Cool, P. and Vansant, E. F., "Synthesis of siliceous materials with micro- and mesoporosity", *Microporous Mesoporous Mater.*, **104**, 26 (2007).

[30] He, Y. L. and Xie, T., "Advances of thermal conductivity models of

nanoscale silica aerogel insulation material", *Appl. Therm. Eng.*, **81**, 28 (2015).

[31] Hou, C. H., Huang, S. C., Chou, P. H. and Den, W., "Removal of bisphenol A from aqueous solutions by electrochemical polymerization on a carbon aerogel electrode", *J. Taiwan Inst. Chem. Eng.*, **51**, 103 (2015).

[32] Liu, H., Sha, W., Cooper, A. T. and Fan, M., "Preparation and characterization of a novel silica aerogel as adsorbent for toxic organic compounds", *Colloids Surf., A: Physicochem. Eng. Aspects*, **347**, 38 (2009).

[33] Domınguez, M., Taboada, E., Molins, E. and Llorca, J., "Co–SiO_2 aerogel-coated catalytic walls for the generation of hydrogen", *Catal. Today*, **138**, 193 (2008).

[34] Sabri, F., Marchetta, J. and Smith, K. M., "Thermal conductivity studies of a polyurea cross- linked silica aerogel-RTV 655 compound for cryogenic propellant tank applications in space", *Acta. Astronautica*, **91**, 173 (2013).

[35] Burchell, M. J., Fairey, S. A. J., Foster, N. J. and Cole, M. J., "Hypervelocity capture of particles in aerogel: Dependence on aerogel properties", *Planetary and Space Sci.*, **57**, 58 (2009).

[36] Wang, C. T. and Wu, C. L., "Electrical sensing properties of silica aerogel thin films to humidity", *Thin Solid Films*, **496**, 658 (2006).

[37] Wang, C. T., Wu, C. L., Chen, I. C. and Huang, Y. H., "Humidity sensors based on silica nanoparticle aerogel thin films", *Sens. Actuators B: Chemical*, **107**, 402 (2005).

[38] Jin, Y., Wu, M., Zhao, G. and Li, M., "Photocatalysis-enhanced electrosorption process for degradation of high-concentration dye wastewater on TiO_2 /carbon aerogel", *Chem. Eng. J.*, **168**, 1248 (2011).

[39] Lin, Y. F. and Chen, J. L., "Magnetic mesoporous Fe/carbon aerogel structures with enhanced arsenic removal efficiency", *J. Colloid Interface Sci.*, **420**, 74 (2014).

[40] Mohammadi, A. and Moghaddas, J. S., "Synthesis, adsorption and regeneration of nanoporous silica aerogel and silica aerogel-activated carbon composites", *Chem. Eng. Res. Des.*, **94**, 475 (2015).

[41] Standeker, S., Novak, Z. and Knez, Z., "Removal of BTEX vapours from waste gas stream using silica aerogels of different hydrophobicity", *J. Hazard. Mater.*, **165**, 1114 (2009).

[42] Rao, A. V., Bhagat, S. D., Hirashima, H. and Pajonk, G. M., "Synthesis of flexible silica aerogels using methyltrimethoxysilane (MTMS) precursor", *J. Colloid Interface Sci.*, **300**, 279 (2006).

[43] Qiu, H., LV, L., Pan, B., Zhang, Q. J., Zhang, W. and Zhang, Q. X., "Critical review in adsorption kinetic models", *J. Zhejiang University Science*, **10** (5), 716 (2015).

[44] Loganathan, S., Tikmani, M., Edubilli, S., Mishra, A. and Ghoshal, A. K., "CO_2 adsorption kinetics on mesoporous silica under wide range of pressure and temperature", *Chem. Eng. J.*, **256**, 1 (2014).

[45] Chauveau, R., Grévillot, G., Marsteau, S. and Vallières, C., "Values of the mass transfer coefficient of the linear driving force model for VOC adsorption on activated carbons", *Chem. Eng. Res. Des.*, **91**, 955 (2013).

[46] Xu, J. and Zhang, J. S., "An experimental study of relative humidity effect on VOCs' effective diffusion coefficient and partition coefficient in a porous medium", *Buil. Env.*, **46**, 1785 (2011).

[47] Crittenden, B. and Thomas, W. J., Adsorption technology and design, 1st ed., Linacre House, Jordan Hill, Oxford, p. 86 (1998).

[48] Peia, J. and Zhang, J. S., "Determination of adsorption isotherm and diffusion coefficient of toluene on activated carbon at low concentrations", *Buil. Env.*, **48**, 66 (2012).

[49] Cao, Y., Zhao, Y., Lv, Z., Song, F. and Zhong, Q., "Preparation and enhanced CO_2 adsorption capacity of UiO-66/grapheme oxide composites", *J. Ind. Eng. Chem.*, **27**, 102 (2015).

[50] Munusamy, K., Sethia, G., Patil, D. V., Rallapalli, P. B. S., Somani, R. S. and Bajaj, H. C., "Sorption of carbon dioxide, methane, nitrogen and carbon monoxide on MIL-101(Cr): Volumetric measurements and dynamic adsorption studies", *Chem. Eng. J.*, **195-196**, 359 (2012).

[51] Gil, M. V., Álvarez-Gutiérrez, N., Martínez, M., Rubiera, F., Pevida, C. and Morán, A., "Carbon adsorbents for CO_2 capture from bio-hydrogen and biogas streams: Breakthrough adsorption study", *Chem. Eng. J.*, **269**, 148 (2015).

[52] Soto, M. L., Moure, A., Domínguez, H. and Parajó, J. C., "Recovery, concentration and purification of phenolic compounds by adsorption: A review", *J. Food Eng.*, **105**, 1 (2011).

[53] Rao, A. P., Rao, A. V. and Pajonk, G. M., "Hydrophobic and physical properties of the ambient pressure dried silica aerogels with sodium silicate precursor using various surface modification agents", *Appl. Surf. Sci.*, **253**, 6032 (2007).

[54] Shi, F., Wang, L. and Liu, J., "Synthesis and characterization of silica aerogels by a novel fast ambient pressure drying process", *Mat. Lett.*, **60**, 3718 (2006).

[55] Lakea, C. B. and Rowe, R. K., "A comparative assessment of volatile organic compound (VOC) sorption to various types of potential GCL bentonites", *Geotext. Geomembr.*, **23**, 323 (2005).

[56] Li, F. and Niu, J., "Simultaneous estimation of VOCs diffusion and partition coefficients in building materials via inverse analysis", *Buil. Env.*, **40**, 1366 (2005).

[57] Luoa, R. and Niu, J. L., "Determining diffusion and partition coefficients of VOCs in cement using one FLEC", *Buil. Env.*, **41**, 1148 (2006).